ISSN (ONLINE): 2454-9762
ISSN (PRINT): 2454-9762
Available online at www.ijarmate.com

International Journal of Advanced Research in Management, Architecture, Technology and Engineering
(IJARMATE) Vol. 3, Special Issue 1, February 2017

LUNG LESION EXTRACTION USING IMPROVED TOBOGGAN BASED REGION GROWING ALGORITHM

[1]K.Vijila Rani

[1]PG Scholar, Dept.of ECE, Arunachala College of Engineering for women
Tamil Nadu
Vijilarani.k@gmail.com

Abstract—Lung cancer is the leading cause of cancer death in both men and women. The accurate segmentation of lung lesion from computerized axial tomography (CAT) scans is important for lung cancer diagnosis and research. A novel toboggan based region growing algorithm with a three-step framework is used for lung lesion segmentation. The initial seed point in the lung lesion was first automatically selected using an improved toboggan method for the subsequent 3D lesion segmentation. Then, the lesion was extracted by an automatic growing algorithm with multi constraints. Finally, the segmentation result was optimized by a lung lesion refining method. By using this lung lesion segmentation algorithm better performance and accuracy will be obtained. In conclusion, we believe that the novel toboggan based region growing algorithm can achieve robust, efficient and accurate lung lesion segmentation in CT images automatically.

Index Terms— Back-off mechanism, computed tomography (CT), lung lesion segmentation, region growing, improved toboggan algorithm

I. INTRODUCTION

LUNG cancer is the leading cause of cancer mortality around the world [1]. Up to 10 million patients in the world will die of lung cancer by 2030 in terms of the report from the World Health Organization [2]. Early prevention of lung tumor has an important role for survival benefit improvements. With the hypothesis that deep analysis of radiographic images can inform and quantify the microenvironment and the extent of intra- tumoral heterogeneity for personalized medicine [3], [4], analysis of large numbers of image features extracted from computed tomography (CT) with high throughput can capture spatial and temporal genetic heterogeneity in a non-invasive way, which is better than invasive biopsy based molecular assays.

ISSN (ONLINE): 2454-9762
ISSN (PRINT): 2454-9762
Available online at www.ijarmate.com

It will be useful for medical research, computer-aided diagnosis, radiotherapy and evaluations of surgery outcome as well. For this purpose, accurate segmentation of lung lesions is the pre-requisite. One method for lung lesion segmentation is that experts with experience such as radiologists delineate the lesion manually. It is a difficult task to obtain robust and efficient results for a variety of reasons. First, the experts may overestimate the lesion volume to enclose the whole lesion. Different manual delineations are also varying. Furthermore, the time consumption limits converting CT images to mineable data with high throughput. Therefore a highly robust, efficient and automatic lung lesion segmentation approach is urgently required. However, accurate segmentation of lung lesions by an automatic method is also difficult because the heterogeneity of the lesions. Christo Ananth et al. [7] proposed a principle in which the division is the urgent stage in iris acknowledgment. We have utilized the worldwide limit an incentive for division. In the above calculation we have not considered the eyelid and eyelashes relics, which corrupt the execution of iris acknowledgment framework. As shown in Fig. 1, due to the diversity of lung lesions, current segmentation accuracy is inadequate. The shape, intensity and location of lung lesions change greatly because of the existence of the spatial genetic heterogeneity of various lesions. The intensity of lung lesions is sometimes close to the intensity of vessels, fissures or chest wall (Fig. 1 a (1)–a (3)). But other times it is close to the intensity of lung field, such as ground-glass opacity (GGO) (Fig. 1 c(1)–c(3)), which is a nonspecific finding on CT scans that indicates a partial filling of air spaces by exudate or transudate, as well as interstitial thickening or partial collapse of lung alveoli [5]. Moreover, the influence of the inherent noise in CT images can also be significant. All these facts render that it is very challenging to achieve the precise delineation of lung lesions automatically.

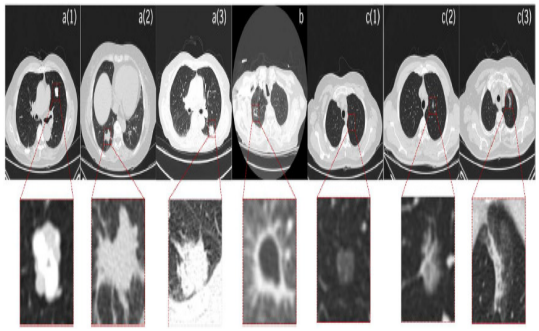

Fig. 1. Different types of lung lesions: (a1)-(a3): solid nodule, a (1): solitary nodule, a (2): juxta vascular, a(3): juxta-pleural, (b): cavity, (c1)-(c3): GGO. c(1): solitary, c(2): juxta-vascular, c(3): juxta-pleural.

II. *Related Work*

Intensity-based segmentation [22], [21] has been applied to the nodule segmentation problem using local density maximum and thresholding algorithms. These classes of algorithms are primarily effective for solitary nodules (well-circumscribed),

ISSN (ONLINE): 2454-9762
ISSN (PRINT): 2454-9762
Available online at www.ijarmate.com

however, fail in separating nodules from juxtaposed surrounding structures, such as the pleural wall (i.e. Juxta-Pleural and Pleural-Tail nodules) and vessels (Vascular), due to their similar intensities. More sophisticated approaches have been proposed to incorporate nodule-specific geometrical and morphological constraints to address this issue (e.g. [23]–[24]). However, juxta-pleural, or wall-attached, nodules still remain a challenge because they can violate geometrical assumptions and appear frequently. In addition, typical low dose CT (LDCT) scans have low contrast, adding further difficulties to obtaining the precise nodule spatial support or region of interest ROI.

In CT slices the rib areas tend to appear with high intensity values, which cause other difficulties when using only intensity-based segmentation approaches. These high-intensity regions near a given marker can bias the semi-automatic nodule center estimator resulting in inaccurate computations of size. Robust segmentation of the juxta-pleural cases can be addressed in two approaches: a) global lung or rib segmentation and b) local non-target removal or avoidance [25]. The first can be effective but also computationally complex and dependent on the accuracy of the whole-lung segmentation. The second is more efficient than the former but more difficult to achieve high performance due to the limited amount of information available for the non-target structures.

II.LESION SEGMENTATION WITH MULTI CONSTRAINTS

Seed point is selected automatically in the lung lesion regions we obtained in section .The multi-constraints are proposed to control the lesion segmentation. As the intensity of vessels and visceral pleura is close to that of the lung lesion, they are sometimes considered to be part of the adjacent lesions.

In the process of lesion segmentation, a five-dimensional symbol vector is defined to describe the new lesion voxels in each generation. The vector is organized by spatial coordinates, iDegree and iCount of each voxel. As the basic flag of growing segmentation, iDegree describes the generation number during segmentation. The initial seed point is the first generation, where the iDegree is given as 1.

On the basis of the area of the lung lesion we have obtained by the improved toboggan algorithm, a largest distance constraint *(LDC)* is defined to restrict the growth in each direction during lesion segmentation. Its morphologic meaning is the maximum Euclidean distance between the center point and lesion boundary points.

The *LDC* we use is calculated as follows:

$$LDC = \sqrt{\frac{Area}{PI}} * Range$$

ISSN (ONLINE): 2454-9762
ISSN (PRINT): 2454-9762
Available online at www.ijarmate.com

Where is the size of the lung lesion region obtained by the improved toboggan algorithm. A decision mechanism of voxel p based on the two-norms is described as follows:

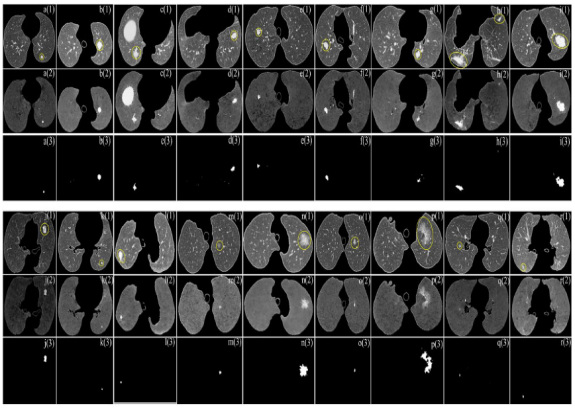

Fig 2. Segmentation by the improved toboggan method, images a to l are solid nodules, and images m to r are ground-glass opacities (GGO).

III .LUNG LESION REFINEMENT

A lung lesion refining method is used for more accurate lesion boundary definition. Since the iterative growing segmentation only uses gray scale information but neglects the morphologic characteristics of the lesion, miniscule incorrect segmentation In the two adjacent lesion slices, for example, one slice includes a slender vessel but its adjacent slice does not[8].

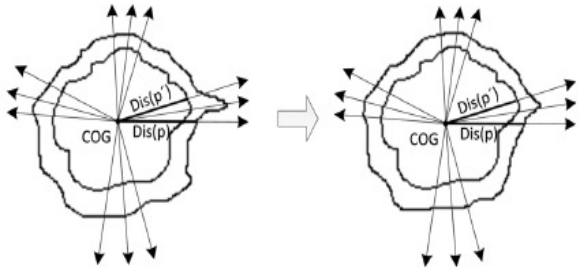

Fig. 3. Lung lesion refining, where the internal profile represents the center image, and the external one represents the adjacent slice.

(a) Presents two contours before boundary smoothing.

(b) Denotes the contours after boundary refining.

The refining method only works on the adjacent lesion slices in a cross-section view, so the two slices being processed are regarded as the center slice *Cl* and its adjacent slice is *Cl'*. The direction from the neck to the abdomen is considered as the main direction.

IV.PROPOSED METHOD

Improved Toboggan Based Region Growing Algorithm is proposed.

ISSN (ONLINE): 2454-9762
ISSN (PRINT): 2454-9762
Available online at www.ijarmate.com

International Journal of Advanced Research in Management, Architecture, Technology and Engineering
(IJARMATE) Vol. 3, Special Issue 1, February 2017

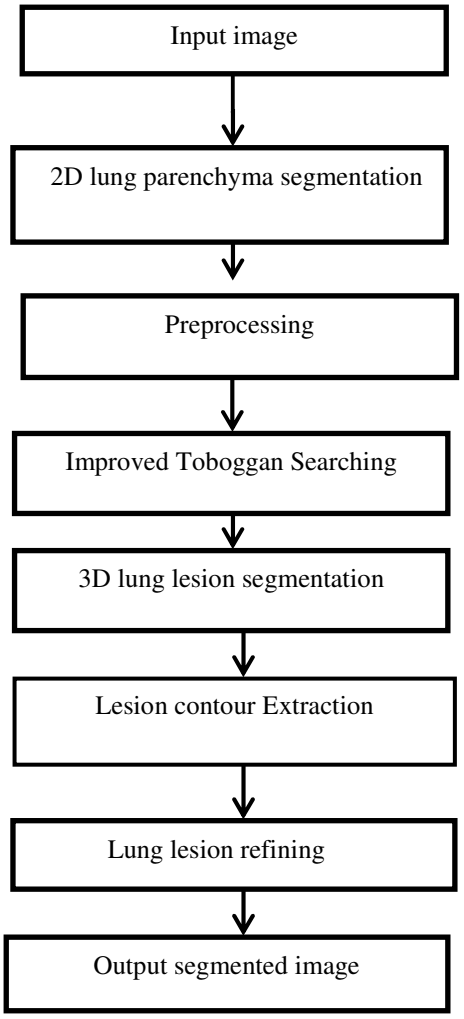

Fig:4. Proposed method Block diagram

a)INPUT IMAGE

Lung lesions from the LIDC-IDRI database were used. The slice thicknesses for those images ranged from 1.25 to 2.50 mm with a 0.70 mm x 0.70 mm resolution. Since their morphology is completely different from that of a solid nodule and GGO. Their diameter ranged from 3 mm to 30 mm (average 9.80 mm).

Fig 5. LIDC database CT scan image

b)2D LUNG PARENCHYMA SEGMENTATION

Image segmentation is the process of partitioning a digital image into multiple segments (sets of pixels, also known as super-pixels). The goal of segmentation is to simplify and/or change the representation of an image into something that is more meaningful and easier to analyze.[12] Image segmentation is typically used to locate objects and boundaries (lines, curves, etc.) in images.

More precisely, image segmentation is the process of assigning a label to every pixel in an image such that pixels with the same label share certain characteristics.[12] Region boundaries and edges are closely

ISSN (ONLINE): 2454-9762
ISSN (PRINT): 2454-9762
Available online at www.ijarmate.com

related, since there is often a sharp adjustment in intensity at the region boundaries. Edge detection techniques have therefore been used as the base of another segmentation technique. The edges identified by edge detection are often disconnected. To segment an object from an image however, one needs closed region boundaries. The desired edges are the boundaries between such objects or spatial-taxons.

c) PREPROCESSING

Image-specific preprocessing methods are aware of the 2-D image nature of the data and are applied two-dimensionally. Dilation of a binary (0/1, 'off'/'on') image expands contiguous regions of 'on' pixels in an image. It examines the neighboring pixels within a 'Window' around each pixel. If more than the specified fraction ('Threshold') of neighboring pixels are 'on' then dilation turns the pixel 'on'. Pixels which are 'on' already are never altered.

Erosion of a binary (0/1, 'off'/'on') image contracts contiguous regions of 'on' pixels in an image. It examines the neighboring pixels within a specified 'Window'. If more than the specified fraction ('Threshold') of neighboring pixels are 'off' then erosion turns the pixel 'off'. Pixels which are 'off' already are never altered.

d) IMPROVED TOBOGGAN SEARCHING

Multi-scale Gaussian convolution could reflect image gradient changes in different directions. For example, different Gaussian convolution kernels could describe the gradient on each coordinate axis (X-axis, Y-axis or Z-axis) in and The multi-scale Gaussian gradient could also give a more accurate description for the lung image compared with other gradient computation methods. Besides, the highlighted noise would be eliminated by the improved toboggan algorithm after contrast enhancement using multi-scale Gaussian convolution.

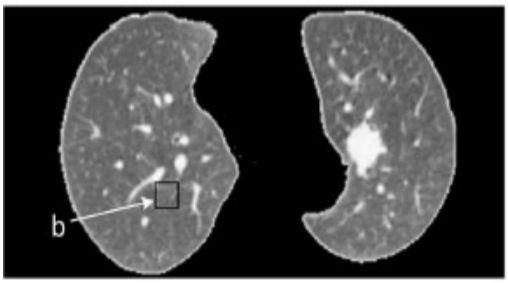

Fig 6. Gradient image of lung parenchyma

By the improved toboggan method, the highlighted vessels, tracheal wall and other noise in the gradient image will be moved into the lung field while the lesion remains at a higher value. Therefore, the other tissues would be dimmed and the lesion could be enhanced in the label image for the subsequent automatic seed point selection.

Algorithm:

Step 1: Calculate the gradient image.

ISSN (ONLINE): 2454-9762
ISSN (PRINT): 2454-9762
Available online at www.ijarmate.com

International Journal of Advanced Research in Management, Architecture, Technology and Engineering
(IJARMATE) Vol. 3, Special Issue 1, February 2017

Step 2: Scan the four neighborhoods (or eight) of each pixel in the gradient image. As one slice is enough for the selection of the lesion seed point.

Step 3: Mark the pixels slide to the local minimum by the same label with the "minimum" pixel.

Step 4: Repeat the process for all pixels. If a pixel is not labeled, its four neighborhoods (or eight) will be searched to find the local minimum. The process is repeated until all pixels in the image are segmented.

e) 3D LUNG LESION SEGMENTATION

Region growing methods rely mainly on the assumption that the neighboring pixels within one region have similar values. The common procedure is to compare one pixel with its neighbors. If a similarity criterion is satisfied, the pixel can be set to belong to the cluster as one or more of its neighbors. The selection of the similarity criterion is significant and the results are influenced by noise in all instances.

One region-growing method is the seeded region growing method[10]. This method takes a set of seeds as input along with the image. The seeds mark each of the objects to be segmented. The regions are iteratively grown by comparison of all unallocated neighboring pixels to the regions. The difference between a pixel's intensity value and the region's mean, r, is used as a measure of similarity. The pixel with the smallest difference measured in this way is assigned to the respective region. This process continues until all pixels are assigned to a region. Because seeded region growing requires seeds as additional input, the segmentation results are dependent on the choice of seeds, and noise in the image can cause the seeds to be poorly placed.

f) LESION CONTOUR EXTRACTION AND LUNG LESION REFINING

Abnormal tissue region are extracted.Lung lesion refining method is used for more accurate lesion boundary definition. Since the iterative growing segmentation only uses grayscale information but neglects the morphologic characteristics of the lesion, miniscule incorrect segmentation .

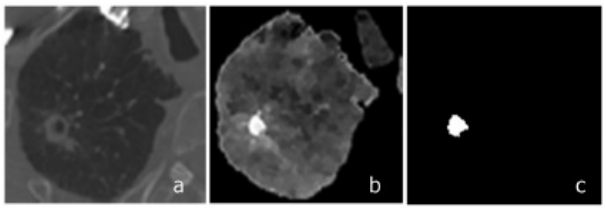

Fig 7. The toboggan results for a cavity tumor.

In the two adjacent lesion slices, for example, one slice includes a slender vessel but its adjacent slice does not. It is displayed as a mutation on the original transverse images. In this section, those mutations will be smoothed for accuracy improvement. Here we use the lesion boundaries in each slice. The refining method in this paper only works on the adjacent lesion slices in a cross-section view, so the two slices being

ISSN (ONLINE): 2454-9762
ISSN (PRINT): 2454-9762
Available online at www.ijarmate.com

processed are regarded as the center slice *Cl* and its adjacent slice is *Cl'*.

The steps of the lung lesion refining method are described as follows:

Step1: Calculate the center of the gravity *(COG,* or a center point in the lesion) in *Cl*:

$$COG = \frac{\sum_{i=1}^{M} CI_i}{M}$$

Where denotes the number of lesion pixels in and represents the coordinate of the lesion points.

Step 2: Extract the lesion contour

Step 3: Compute the distance between *COG* and the boundary point 6* *on Cl:*

$$Dis(b_i) = \|b_i - COG\|_2, i = (0, 1 \ldots n)$$

Where \\h - *COG*\\$_2$ means the two-norms of *(b_uCOG),* and *n* is the total number of boundary points. *Dis(bi)* represents the Euclidean distance from *bi* to *COG.*

Step 4: Calculate the distance between *COG* and the boundary point 6^ on *Cl'*. Draw the straight line which is determined by *COG* to *b'i- DisW* is used to describe the distance:

$$Dis\,(b_i') = \|b_i' - COG\|_2\,, i = (0, 1 \ldots n')$$

Where *n'* represents the boundary points in *Cl'*. On the original transverse images, voxels and are the boundary points of lesion.

We will process each difference between Dis (b) and *Dis (bi)* in the same direction in the next steps.

Step5: Execute Step 4 on all boundary points in *Cl'. Dis)* and *Dis(bi)* in each direction are stored for the subsequent calculation in Step 6.

Step 6: Obtain the average distance *Avg:*

$$Avg = \sum_{points} (\|Dis\,(b_i') - Dis(b_i)\|)\,/points$$

g) OUTPUT SEGMENTED IMAGE

Image contains solid nodule**,** solitary GGO, juxta-pleural GGO. Algorithm significantly improves lung lesion segmentation accuracy compared with other methods.

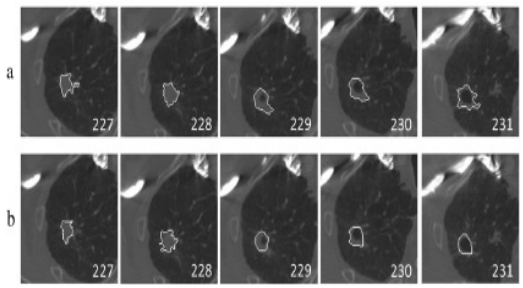

Fig 8. segmentation results of the cavity tumor

V . RESULTS AND DISCUSSION

ISSN (ONLINE): 2454-9762
ISSN (PRINT): 2454-9762
Available online at www.ijarmate.com

International Journal of Advanced Research in Management, Architecture, Technology and Engineering
(IJARMATE) Vol. 3, Special Issue 1, February 2017

a) Input image

An input image taken here is LIDC database CT scan image Shown in below.

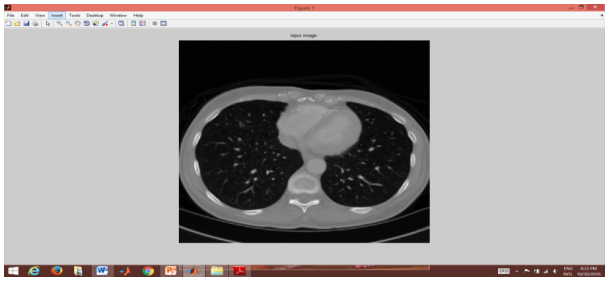

Fig 9. Input image

b)2D lung parenchyma segmentation

The edge of input image is segmented using prewitt method.

Fig 10. 2D lung parenchyma segmentation

c) Preprocessing

Image-specific preprocessing dilation and erosion methods are aware of the 2-D image nature of the data and are applied two dimensionally.

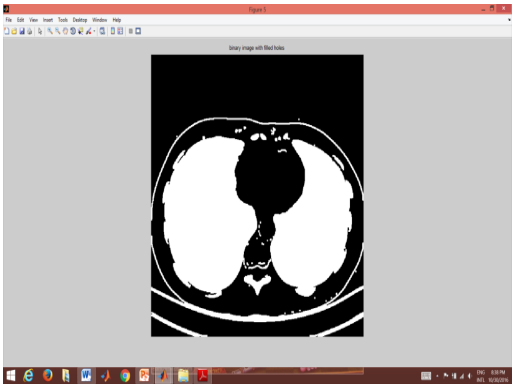

Fig 11. Dilated image

d) Improved Toboggan Searching

By the improved toboggan method, the highlighted vessels, tracheal wall and other noise in the gradient image will be moved into the lung field while the lesion remains at a higher value.

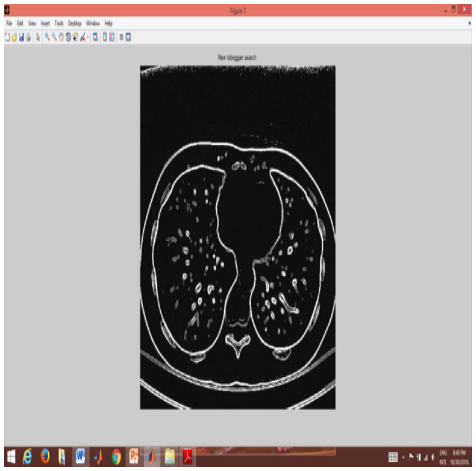

Fig 12. Toboggan search image

e) Segmentation single slice image

Single slice of sensitive segmented image shown in below

ISSN (ONLINE): 2454-9762
ISSN (PRINT): 2454-9762
Available online at www.ijarmate.com

International Journal of Advanced Research in Management, Architecture, Technology and Engineering
(IJARMATE) Vol. 3, Special Issue 1, February 2017

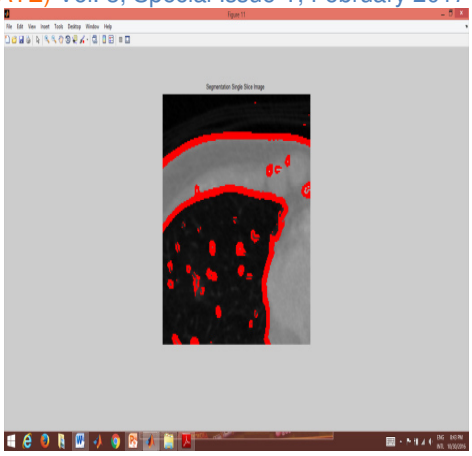

Fig 14. Single slice image

f)3D lung lesion segmentation

One region growing method is the seeded region growing method. This method takes a set of seeds as input along with the image.

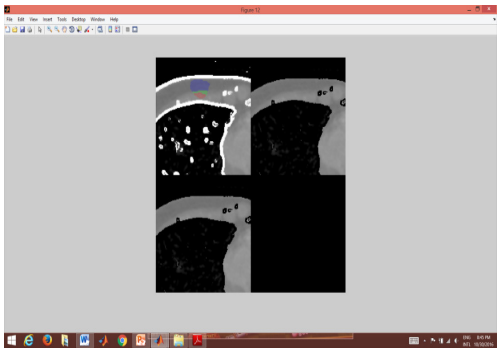

Fig 15. 3D lung lesion segmentation image

g) Lung lesions including solid nodules

Image contains solid nodule**,** solitary GGO, juxta-pleural GGO.

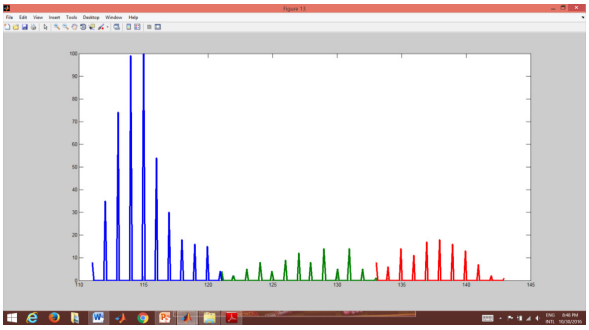

Fig 16. Different types of lung lesion

h) Lesion region of the cavity tumor

Abnormal tissue of lung is said to be cavity tumor that can be shown in below

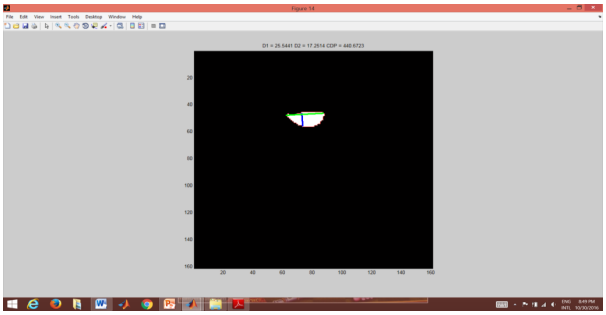

Fig 17. Output segmented cavity tumor region

VI CONCLUSION

This paper explains about an automatic and quick-response lung lesion segmentation algorithm, which has been tested on the public LIDC database. The initial seed points were first detected using an improved toboggan method for the subsequent lesion segmentation. Then, the lesion was extracted by an automatic growing algorithm with multi-constraints. Finally, the segmentation result was

ISSN (ONLINE): 2454-9762
ISSN (PRINT): 2454-9762
Available online at www.ijarmate.com

optimized by a lung lesion refining method. The important component of this work is that it does not require any training datasets or human interactions for lesion seed point detection, while it could obtain more accurate segmentation results compared with other methods, especially for ground-glass opacities. Better performance was obtained with improved time efficiency by our method.

FUTURE WORK

As the new method has a variety of advantages for the segmentation of lung lesions and can also be applied as a reference for lesion segmentation in other tissues. In the future classification of the lesions into benign and malignant to be done and calculation of the area and the size of the lesions using simpler algorithms will be addressed.

REFERENCES

[1] *R. Siegel, D. Naishadham, and A. Jemal, "Cancer statistics, 2013," CA Cancer J Clin, vol. 63, pp. 11-30, Jan. 2013.*

[2] *W. H. Organization, "Description of the global burden of NCDs, their risk factors and determinants," Geneva, Switzerland: World Health Organization, 2011.*

[3] *H. J. W. L. Alerts, E. R. Velazquez, R. T. H. Leijenaar, C. Parmer, P. Grossmann, S. Cavalho, J. Bussink, R. Monshouwer, B. Haibe-Kains, Rietveld, F. Hoebers, M. M. Rietbergen, C. R. Leemans, A. Dekker, J. Quackenbush, R. J. Gillies, and P. Lambin, "Decoding tumour phenotype by noninvasive imaging using a quantitative radiomics approach.,"Nat. Commun., vol. 5, p. 4006, 2014.*

[4] *J. Song and C. Yang et al., "A New Quantitative Radiomics Approach for Non-Small Cell Lung Cancer (NSCLC) Prognosis," in presented at the Wind Int. Conf. Radiological Society of North America, Chicago, Illinois, November 29-December 04 2015.*

[5] *M. Nakata, H. Saeki, I. Takata, Y. Segawa, H. Mogami, K. Mandai, and K. Eguchi, "Focal ground-glass opacity detected by low-dose helical CT," Chest, vol. 121, no. 5, pp. 1464-1467, 2002.*

[6] *David S. Paik, Christopher F. Beaulieu, Geoffrey D. Rubin, Burak Acar, R. Brooke Jeffrey, Jr., Judy Yee,Joyoni Dey, and Sandy Napel"Surface Normal*

ISSN (ONLINE): 2454-9762
ISSN (PRINT): 2454-9762
Available online at www.ijarmate.com

overlap: A Computer-Aided Detection algorithm With Application To Colonic Polyps And Lung Nodules In Helical CT", Volume 2, Issue 6, June 2004 , ISSN 2250-3153

[7] *Christo Ananth,"Iris Recognition Using Active Contours",International Journal of Advanced Research in Innovative Discoveries in Engineering and Applications[IJARIDEA],Volume 2,Issue 1,February 2017,pp:27-32.*

[8] *D. Mahapatra, P. J. Schuf, J. a. W. Tielbeek, J. C. Makanyanga], J. Stoker, S. a Taylor, F. M. Vos, and J. M. Buhmann, "Automatic Detection And Segmentation Of Crohn ' S Disease Tissues From Abdominal MRI," IEEE Trans. Med. Imaging,vol. 32, no. 12, pp. 2332-2347, 2013.*

[9] *E. M. Van Rikxoort, B. Lassen, M. Schmidt, S. Kerkstra, B. Van Ginneken,and J. M. Kuhnigk, "Automatic Segmentation Of The Pulmonary Lobes From Chest CT Scans Based On Fissures, Vessels, Bronchi," IEEE Trans. Med. Imaging, vol. 32, no. 2, pp. 210–222, 2013*

[10] *E. a. Hoffman, S. Hu and J. M. Reinhardt, "Automatic Lung Segmen-tation For Accurate Quantitation Of Volumetric X-Ray CT Images," IEEE Trans. Med. Imaging, vol. 20, no. 6, pp. 490^98, 2001.*

[11] *Foster A. Mansoor, U. Bagci, Z. Xu, K. N. Olivier, and J. M. Elinoff et al., "A Generic Approach To Pathological Lung Segmentation," IEEE Trans Med Imaging, vol. 33, pp. 2293–2310, Dec. 2014.*

[12] *Jungian Song "Lung Lesion Extraction Using A Toboggan Based Growing Automatic Segmentation Approach," IEEE Trans Med Imaging, vol. 35, No 1,Jan. 2016.*

[13] *J. H. Graham, and A. a Farag, H. E. A. El Munim "A Novel Approach For Lung Nodules Segmentation In Chest CT Using Level Sets.," IEEE Trans. Image Process., vol. 22, no. 12, pp. 5202-5213, 2013.*

[14] *J. Cornelis M. Tan, R. Deklerck, B. Jansen, M. Bister, "A Novel Computer-Aided Lung Nodule Detection System For Ct Images," Med. Phys., vol. 38, no. 10, p. 5630, 2011*

[15] *M. Nakata, H. Saeki, I. Takata, Y. Segawa, H. Mogami, K. Mandai, and K. Eguchi, "Focal ground-glass opacity detected by low-dose helical CT," Chest, vol. 121, no. 5, pp. 1464-1467, 2002.*

[16] *M. Athelogou, G. Schmidt, A. Schape, M. Baatz, and G. Binnig, "Cognition Network Technology - A Novel Multimodal Image Analysis Technique for Automatic Identification and Quantification of Biological Image Contents," Imaging Cellular and*

ISSN (ONLINE): 2454-9762
ISSN (PRINT): 2454-9762
Available online at www.ijarmate.com

Molecular Biological Functions, pp. 407-422, 2007.

[17] *Q. Wang, E. Song, R. Jin, P. Han, X. Wang, Y. Zhou, and J. Zeng, "Segmentation of lung nodules in computed tomography images using dynamic programming and multidirectional fusion techniques.," Acad. Radiol., vol. 16, no. 6, pp. 678-688, 2009.*

[18] *R. Siegel, D. Naishadham, and A. Jemal, "Cancer statistics, 2013," CA Cancer J Clin, vol. 63, pp. 11-30, Jan. 2013.*

[19] *S. Candemir, S. Jaeger, K. Palaniappan, J. P. Musco, R. K. Singh, Z. Xue, A. Karargyris, S. Antani, G. Thoma, segmentation in chest radiographs using anatomical atlases with nonrigid registration," IEEE Trans. Med. Imaging, vol. 33, no. 2, pp. 577-590, 2014.*

[20] *S. Diciotti, G. Picozzi, M. Falchini, M. Mascalchi, N. Villari, and G. Valli, "3-D segmentation algorithm of small lung nodules in spiral CT images.," IEEE Trans. Inf. Technol. Biomed., vol. 12, no. 1, pp. 7-19, 2008.*

[21] *C.Li, R. Huang, Z. Ding, J. C. Gatenby, D. N. Metaxas, and J. C. Gore, "A Level Set Method For Image Segmentation In The Presence Ofin- Tensity Inhomogeneities With Application To MRI" ,IEEE Trans. Image Process., vol. 20, no. 7, pp. 2007-2016, 2011.*

[22] B. Zhao, D. Yankelevitz, A. Reeves, and C. Henschke, "Two-dimensional multi-criterion segmentation of pulmonary nodules on heli-cal CT images," Med. Phys., vol. 26, no. 6, pp. 889–895, Jun. 1999.

[23] W. J. Kostis, D. F. Yankelevitz, I. Henschke, "Small pulmonary nodules: Reproducibility of three-dimensional volumetric measurement and estimation of time to follow-up," Radiology, Vol. 231, pp. 446–52, May 2004.

[24]T. Kubota, A. K. Jerebko, M. Dewan, M. Salganicoff, and A. Krishnan, "Segmentation of pulmonary nodules of various densities with morpho-logical approaches and convexity models," Med. Image Anal., vol. 15, no. 1, pp. 133–154, Feb. 2011.

[25] J. P. Ko, H. Rusinek, E. L. Jacobs, J. S. Babb, M. Betke, G. McGuinness, and D. P. Naidich, "Small pulmonary nodules: Volume measurement at chest CT—Phantom study," Radiology, vol. 228, pp. 864–870, Sep. 2003.

[26] S. Diciotti, G. Picozzi, M. Falchini, M. Mascalchi, N. Villari, and Valli, "3D segmentation algorithm of small lung nodules in spiral CT Images," IEEE Trans. Inf. Technol. Biomed., vol. 12, no. 1, pp. 7–19, Jan. 2008.

[27]D. Wu, L. Lu, J. Bi, Y. Shinagawa, K. Boyer, A. Krishnan, and Salganicoff1, "Stratified learning of local anatomical context for lung nodules in CT images," in Proc. IEEE Conf. CVPR, Jun. 2010, pp. 2791–2798.

[28]B. Van Ginneken, "Supervised probabilistic segmentation of pulmonary nodules in CT scans," in Proc. 9th Int. Conf. MICCAI, Oct. 2006, pp. 912–919.

[29]K. Okada, V. Ramesh, A. Krishnan, M. Singh, and U. Akdemir, "Robust pulmonary nodule segmentation in CT: Improving performance for juxta pleural cases," in Proc. 8th Int. Conf. MICCAI, Oct. 2005, pp. 781–789.
[30]J. Dehmeshki, H. Amin, M. Valdivieso, and X. Ye, "Segmentation of pulmonary nodules in thoracic CT scans: A region growing approach," IEEE Trans. Med. Imaging, vol. 27, no. 4, pp. 467–480, Apr. 2008.

